# Wiener Feedback Filtering for Suppression of Residual ISI and Correlated Noise in MC-CDMA

Haibing Yang[1] and Jean-Paul M. G. Linnartz[1,2]
[1]Radio Communications Group (TTE-ECR), Eindhoven University of Technology, Eindhoven, The Netherlands
[2]Connectivity Systems and Networks (CoSiNe), Philips Research, Eindhoven, The Netherlands
email: h.yang@tue.nl and j.p.linnartz@philips.com

***Abstract*— Multi-carrier CDMA takes advantage of frequency diversity by spreading each user symbol across multiple subcarriers to improve the transmission performance. However, the performance of linear detection schemes is affected by the residual inter-symbol interference (ISI) and the correlated noise present in decision variables. In order to improve the performance, a decision feedback equalization (DFE) scheme is proposed in this paper. In the feedback stage, an optimal Wiener filter is designed to predict and suppress the residual ISI and the correlated noise caused by the channel equalization and code despreading in the feedforward stage. Simulations show that the proposed DFE scheme significantly outperforms the conventional linear minimum mean-square error (MMSE) receiver. By this scheme, a noise penalty between MC-CDMA and ideally coded OFDM is largely reduced.**

## I. Introduction

The modulation method of multi-carrier code division multiple access (MC-CDMA) based on the orthogonal frequency division multiplexing (OFDM) technique is interesting for low-complexity and high-data-rate transmission in wireless local area networks [1], [2]. Basically, the user symbols are spread over multiple subcarriers with the aid of spreading codes, such as the Walsh-Hadamard code that will be considered in this paper, prior to the inverse fast Fourier transform (IFFT). By spreading the symbols across the whole spectrum, MC-CDMA takes advantage of frequency diversity and is thus robust to frequency selectivity in multipath dispersive environments.

In conventional MC-CDMA, linear receiver schemes have been applied for signal detection in the receiver, where various strategies are considered for designing the equalization matrix in the receiver [2]–[5]. Among these, the linear receiver scheme based on minimum-mean-square error (MMSE) criterion outperforms those based on maximum ratio combining (MRC) and zero-forcing (ZF) [4], [6]. The MMSE scheme compromises the noise enhancement and symbol distortion, and eventually achieves the best performance among these schemes. However, the linear MMSE equalization and the consecutive code despreading in MC-CDMA lead to residual inter-symbol interferences (ISI) and correlated noises in decision variables, which degrades the system performance. This results in channel capacity loss, compared with ideally coded OFDM as noticed in [2]. This current paper will show that this penalty vanishes if the noise correlation is removed.

In order to suppress such residual ISI and the correlated noise, we propose a decision feedback equalizer (DFE) in this paper. The concept of DFE has been applied in many applications, such as in single-carrier transmission and OFDM [7]–[9], but this is to our knowledge the first time to use DFE in MC-CDMA. In the proposed scheme, a one-tap frequency domain equalizer is realized in the feedforward stage and a Wiener prediction filter is designed in the feedback stage to estimate the residual ISI and the correlated noise. The feedback stage is realized in the code domain, which is after the code despreading. As will be seen, this scheme provides a significant performance improvement, compared with the linear MMSE detection scheme.

## II. System model

In this section, we describe a baseband equivalent MC-CDMA system. Here we address the synchronous downlink for one user using the whole spreading code matrix. In the transmitter, user symbols are packed into data blocks with length $N$ and each block is linearly transformed by a Walsh-Hadamard code matrix before an IFFT operation. For convenience, we only consider one block denoted as $\boldsymbol{x} = [x_0, x_1, \cdots, x_{N-1}]^T$, where each data symbol is independent from others and has the energy $E_s$, i.e. $E\{\boldsymbol{x}\boldsymbol{x}^H\} = E_s\boldsymbol{I}$. After Walsh-Hadamard transform (WHT) and IFFT, the resulting signal block is written as

$$\boldsymbol{u} = \boldsymbol{F}^H\boldsymbol{C}\boldsymbol{x}, \tag{1}$$

with $\boldsymbol{u} = [u_0, u_1, \cdots, u_{N-1}]^T$, where $^H$ denotes the complex transpose, $\boldsymbol{F}$ is the $N \times N$ matrix performing FFT operation and $\boldsymbol{C}$ is a Walsh-Hadamard code matrix performing WHT operation. The code matrix is built with the elements

$$C_{m,n} = \frac{1}{\sqrt{N}} \prod_{i=0}^{N-1} (-1)^{m_i n_i}, \tag{2}$$

where $m = \sum_{i=0}^{N-1} m_i 2^i$, $n = \sum_{i=0}^{N-1} n_i 2^i$ and $m_i, n_i \in \{0, 1\}$ are the binary representations of $m$ and $n$, respectively. Both $\boldsymbol{F}$ and $\boldsymbol{C}$ are unitary matrices satisfying $\boldsymbol{F}\boldsymbol{F}^H = \boldsymbol{I}$ and $\boldsymbol{C}\boldsymbol{C}^H = \boldsymbol{I}$, respectively, where $\boldsymbol{I}$ is an identity matrix. This suggests that the matrices $\boldsymbol{F}^H$ and $\boldsymbol{C}^H$ perform IFFT and inverse WHT (IWHT) operations, respectively.

Next to the IFFT, a cyclic prefix is inserted in the front of the signal block and then the signal block is transmitted in a time invariant multipath dispersive channel with the channel length $L+1$. Without loss of generality, we assume that the length of the cyclic prefix is always larger than the channel length. In this way, the inter-block interference can be completely resolved by the cyclic prefix.

In the receiver, we assume that the time and frequency synchronizations of the signal are perfect and that the cyclic prefix is removed. Then the received signal block before FFT is $\boldsymbol{r} = [r_0, r_1, \cdots, r_{N-1}]^T$, in which the entries are the circular convolution of the transmitted signal and the channel impulse response contaminated by the noise, i.e.

$$r_n = \sum_{l=0}^{L} h_l u_{(n-l) \bmod N} + v_{t,n}. \tag{3}$$

Here $\{h_l\}$ are the taps of the channel impulse response and $\{v_{t,n}\}$ are independently and identically distributed ($i.i.d.$) zero mean additive white Gaussian noise (AWGN) with variance $N_0$. For a Rician fading channel, the first tap $h_0$ is fixed and other taps are $i.i.d.$ complex Gaussian distributed. Rewriting (3) into the vector form leads to

$$\boldsymbol{r} = \text{cir}\{\boldsymbol{h}\}\boldsymbol{u} + \boldsymbol{v}_t, \tag{4}$$

where the noise $\boldsymbol{v}_t = [v_{t,0}, v_{t,1}, \cdots, v_{t,N-1}]^T$ and the channel matrix cir$\{\boldsymbol{h}\}$ is an $N \times N$ circulant matrix with the first column $\boldsymbol{h} = [h_0, h_1, \cdots, h_L, 0, \cdots, 0]^T$.

The received signal after FFT may be written as

$$\boldsymbol{y} = \boldsymbol{H}\boldsymbol{C}\boldsymbol{x} + \boldsymbol{v}, \tag{5}$$

where $\boldsymbol{y} = [y_0, y_1, \cdots, y_{N-1}]^T$, the noise in frequency domain is $\boldsymbol{v} = \boldsymbol{F}\boldsymbol{v}_t$ and the channel matrix in frequency domain $\boldsymbol{H} = \boldsymbol{F}\text{cir}\{\boldsymbol{h}\}\boldsymbol{F}^H$. Notice that the noise $\boldsymbol{v}$ in frequency domain is $i.i.d.$ and follows the same nature as $\boldsymbol{v}_t$. Since the channel considered in this paper is time invariant, the matrix $\boldsymbol{H}$ is diagonal and the $n$the diagonal element, $H_n = \sum_{k=0}^{N-1} h_k e^{-j2\pi kn/N}$, represents the complex attenuation of the channel at the $n$th subcarrier. The signal at each subcarrier is equalized to remove the effect of the channel and the equalized signal is then transformed by inverse WHT so that the user symbols can be detected.

## III. Conventional MMSE detection

A conventional MMSE equalizer can be applied in the receiver to equalize the signal attenuation at each subcarrier prior to code despreading. In detail, the signal vector $\boldsymbol{y}$ is weighed by a weight matrix $\boldsymbol{W}$ prior to the code despreading. Since the considered channel is time invariant, the MMSE weight matrix is a diagonal matrix with the $n$th diagonal element $W_n = \frac{H_n^*}{|H_n|^2 + N_0/E_s}$, where the channel attenuation $H_n$ is known in the receiver. By minimizing the mean-square error between the equalized signal and the desired signal, the MMSE equalizer compromises the noise enhancement and the symbol distortion. The resulting equalized signal after code despreading, $\boldsymbol{s} = [s_0, s_1, \cdots, s_{N-1}]^T$, consists of the desired signal $\boldsymbol{x}$ and the error signal $\boldsymbol{e} = [e_0, e_1, \cdots, e_{N-1}]^T$, i.e.

$$\boldsymbol{s} = \boldsymbol{x} + \underbrace{\boldsymbol{C}^H(\boldsymbol{W}\boldsymbol{H} - \boldsymbol{I})\boldsymbol{C}\boldsymbol{x} + \boldsymbol{C}^H\boldsymbol{W}\boldsymbol{v}}_{\boldsymbol{e}}, \tag{6}$$

which are then fed into a detection device for the recovery of user symbols. The error signal $\boldsymbol{e}$ consists of the residual ISI $\boldsymbol{C}^H(\boldsymbol{W}\boldsymbol{H} - \boldsymbol{I})\boldsymbol{C}\boldsymbol{x}$, and the correlated noise $\boldsymbol{C}^H\boldsymbol{W}\boldsymbol{v}$. The error signal occurs because the signal and noise components at different subcarriers are combined into each decision variable by the code despreading operation, which affects the detection performance and eventually results in channel capacity loss, as discussed in [2].

## IV. DFE design

### A. The proposed DFE structure

To suppress the residual ISI and correlated noise in (6), we adopt a decision feedback structure shown in Fig.1, where the DFE consists of a feedforward equalizer (FFE) in frequency domain and a feedback equalizer (FBE) after code despreading. In the feedforward stage, the FFE matrix $\boldsymbol{W}$ equalizes the complex channel attenuation at each subcarrier. In the feedback stage, the FBE matrix $\boldsymbol{D}$ is used to estimate the residual ISI (if there is) and the correlated noise, which is then removed from the equalized signal after code spreading.

The FBE unit is excited by the sequence $\tilde{\boldsymbol{e}} = \boldsymbol{s} - \hat{\boldsymbol{x}}$, where $\hat{\boldsymbol{x}}$ are the recovered symbols in the feedforward stage. When the symbols are perfectly recovered, i.e. $\hat{\boldsymbol{x}} = \boldsymbol{x}$, the sequence $\tilde{\boldsymbol{e}}$ is the same as the error signal in (6). The output sequences of the FBE unit are the estimated error sequence $\hat{\boldsymbol{e}} = [\hat{e}_0, \hat{e}_1, \cdots, \hat{e}_{N-1}]^T$ based on the observation of $\tilde{\boldsymbol{e}}$, according to $\hat{\boldsymbol{e}} = \boldsymbol{D}\tilde{\boldsymbol{e}}$. With the estimated error removed, a cleaner decision variable, $\boldsymbol{z} = [z_0, z_1, \cdots, z_{N-1}]^T$, is obtained and given by

$$\boldsymbol{z} = \boldsymbol{s} - \hat{\boldsymbol{e}}. \tag{7}$$

It is noteworthy to point out that the DFE structure in Fig.1 is equivalent to the predictive DFE proposed in [10], where both the feedforward and feedback stages are implemented in time domain. The DFE structure has been applied successfully in literature to combat ISI and correlated noise [10]–[12]. A recent application is in single carrier block systems [8], where the DFE is used to suppress the residual ISI and correlated noise caused by the inverse FFT of the equalized signal that is similar to the problem here. As will be shown later, the advantage of this type of DFE structure is that adjusting the number of taps in the feedback stage will not affect the weight matrix in the feedforward stage, in contrast to the decision directed DFE. This motivates the adoption of the DFE structure in this paper.

### B. MMSE-DFE Equalizer design

Now we concentrate on the equalizer design for the receiver structure in Fig.1. The input signal of the decision device is

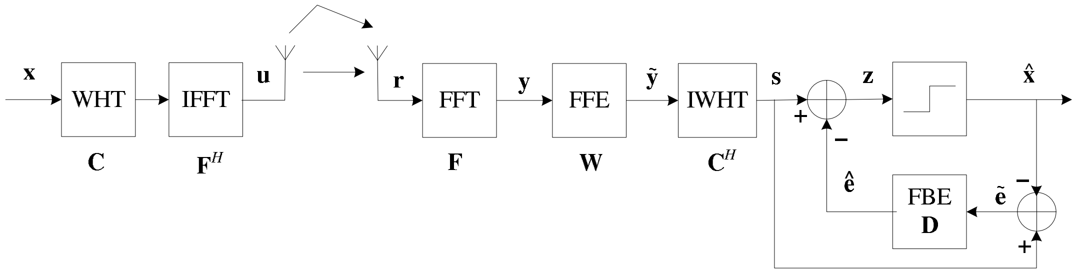


Fig. 1. MC-CDMA transmitter and the proposed DFE receiver structure.

$\boldsymbol{z} = \boldsymbol{s} - \boldsymbol{D}\tilde{\boldsymbol{e}} = (\boldsymbol{I} - \boldsymbol{D})\boldsymbol{s} + \boldsymbol{D}\hat{\boldsymbol{x}}$ and the error vector of the input signal is given by

$$\boldsymbol{\epsilon} = \boldsymbol{z} - \boldsymbol{x} = (\boldsymbol{I} - \boldsymbol{D})(\boldsymbol{s} - \boldsymbol{x}), \tag{8}$$

where the feedback symbols have been assumed to be always correct, i.e. $\hat{\boldsymbol{x}} = \boldsymbol{x}$. Then the autocorrelation matrix will be

$$\begin{aligned} E\{\boldsymbol{\epsilon}\boldsymbol{\epsilon}^H\} &= (\boldsymbol{I} - \boldsymbol{D})E\{(\boldsymbol{s} - \boldsymbol{x})(\boldsymbol{s} - \boldsymbol{x})^H\}(\boldsymbol{I} - \boldsymbol{D})^H \\ &= E_s(\boldsymbol{I} - \boldsymbol{D})\boldsymbol{C}^H \\ &\quad \cdot(\boldsymbol{W}\boldsymbol{T}\boldsymbol{W}^H - \boldsymbol{W}\boldsymbol{H} - \boldsymbol{H}^H\boldsymbol{W}^H + \boldsymbol{I}) \\ &\quad \cdot\boldsymbol{C}(\boldsymbol{I} - \boldsymbol{D})^H, \end{aligned} \tag{9}$$

where the matrix

$$\boldsymbol{T} = \boldsymbol{H}\boldsymbol{H}^H + \frac{N_0}{E_s}\boldsymbol{I}. \tag{10}$$

Now the coefficients of the feedforward and feedback equalizers can be derived by minimizing the mean squared error (MSE), which is the trace of (9).

First, by setting the derivative of the trace of (9), with respect to the equalization matrix $\boldsymbol{W}$, to be zero, we obtain the optimal MMSE weight

$$\boldsymbol{W}_{\text{opt}} = \boldsymbol{H}^H\boldsymbol{T}^{-1}. \tag{11}$$

Note that for the time invariant channel, the solution (11) is exactly the same as the conventional one-tap MMSE equalizer given in Section III. Substituting (11) back to (9), we have the autocorrelation matrix

$$E\{\boldsymbol{\epsilon}\boldsymbol{\epsilon}^H\} = (\boldsymbol{I} - \boldsymbol{D})\boldsymbol{C}^H\boldsymbol{Q}\boldsymbol{C}(\boldsymbol{I} - \boldsymbol{D})^H, \tag{12}$$

where $\boldsymbol{Q} = \boldsymbol{I} - \boldsymbol{H}^H\boldsymbol{T}^{-1}\boldsymbol{H}$ is a diagonal matrix with the $n$th diagonal element $Q_n = \frac{N_0/E_s}{|H_n|^2 + N_0/E_s}$.

Next is to derive the optimal FBE matrix $\boldsymbol{D}$. If there is no restriction is imposed on the equalization matrix $\boldsymbol{D}$, the solution to minimize the trace of (12), with respect to $\boldsymbol{D}$, is the identical matrix $\boldsymbol{D}_{\text{opt}} = \boldsymbol{I}$. Then, the input to the decision device are the recovered symbols in the feedback stage, i.e., $\boldsymbol{z} = \hat{\boldsymbol{x}}$. This means that, from the point of view of information theory, the intrinsic information is fed back via the non-zero diagonal elements of $\boldsymbol{D}$, which results in no performance improvement at all. Therefore, similar to the strategy of turbo decoding [13], only extrinsic information should be used to gain the improvement by restricting the diagonal elements of $\boldsymbol{D}$ to be zero. By doing so, the estimation of the residual ISI and the correlated noise merely turns into a prediction problem.

For perfectly recovered symbols in the feedforward stage, the output signal of the FBE unit is $\hat{\boldsymbol{e}} = \boldsymbol{D}\boldsymbol{e}$. With the diagonal elements of $\boldsymbol{D}$ restricted to be zeros, the $n$th entry of $\hat{\boldsymbol{e}}$, $\hat{e}_n$, is the prediction of $e_n$ given by

$$\hat{e}_n = \sum_{\substack{k=0 \\ k \neq n}}^{N-1} D_{n,k} e_k \tag{13}$$

for $0 \leq n \leq N-1$. It is clear that the predicted signal is a linearly weighted combination of the other error signals. Notice that the error sequence $\{e_k\}$ should be replaced in practice by the observed sequence $\{\tilde{e}_k\}$, since $\{e_k\}$ are unknown. Here $D_{n,k}$ is the $(n,k)$th entry of the $N \times N$ feedback matrix $\boldsymbol{D}$ with zero diagonals. The optimal Wiener filter taps $D_{n,k}$ can be attained by minimizing the MSE between $\hat{e}_n$ and $e_n$, which is equivalent to minimize the trace of (12). According to the orthogonality principle for Wiener filter design, we have

$$E\{e_n e_m^*\} = E\{\hat{e}_n e_m^*\}, \qquad (m \neq n) \tag{14}$$

for $m, n \in [0, N-1]$. From (14), the optimal Wiener filter taps $\{D_{n,k}\}$ for predicting the $n$th error signal $e_n$ can be solved. The next step is to derive the explicit expression of (14).

Note that the left and right sides of (14) are the $(n,m)$th entries of the auto- and cross-correlation matrix, $E\{\boldsymbol{e}\boldsymbol{e}^H\}$ and $E\{\hat{\boldsymbol{e}}\boldsymbol{e}^H\}$, respectively. Combining (6), (11), $\boldsymbol{e} = \boldsymbol{s} - \boldsymbol{x}$ and $\hat{\boldsymbol{e}} = \boldsymbol{D}\boldsymbol{e}$, we have the autocorrelation matrix $E\{\boldsymbol{e}\boldsymbol{e}^H\} = \boldsymbol{C}^H\boldsymbol{Q}\boldsymbol{C}$ and the cross-correlation matrix $E\{\hat{\boldsymbol{e}}\boldsymbol{e}^H\} = \boldsymbol{D}\boldsymbol{C}^H\boldsymbol{Q}\boldsymbol{C}$. The $(n,m)$th entries of the auto- and cross-correlation matrix can be derived

$$E\{e_n e_m^*\} = \frac{1}{\sqrt{N}} q_{n \oplus m}, \tag{15}$$

$$E\{\hat{e}_n e_m^*\} = \frac{1}{\sqrt{N}} \sum_{k=0}^{N-1} D_{n,k} q_{k \oplus m}, \tag{16}$$

respectively, where $\oplus$ denotes the modulo-2 addition. Modulo-2 addition is performed using an "exclusive OR (XOR)" operation on the corresponding binary digits of each operand[1]

[1]Modulo-2 addition is both a commutative and an associative operation, i.e.,

$$\text{commutativity:} \quad m \oplus n = n \oplus m \tag{17}$$

$$\text{associativity:} \quad (m \oplus n) \oplus s = m \oplus (n \oplus s) = m \oplus n \oplus s \tag{18}$$

[14]. Here the sequence $\{q_k\}$ is related to the sequence of $\{Q_k\}$, which are the diagonal elements of the diagonal matrix $\boldsymbol{Q}$, by $q_k = \sum_{k'=0}^{N-1} C_{k,k'} Q_k$ for $k = 0, 1, \cdots, N-1$.

Substituting (15) and (16) into (14) and using the associative and commutative properties of modulo-2 addition, we have

$$\sum_{m' \oplus n=1}^{N-1} q_{m \oplus m'} D_{n,m' \oplus n} = q_m \qquad (m, m' \neq 0), \tag{19}$$

which can be further simplified as

$$\sum_{m'=1}^{N-1} q_{m \oplus m'} D_{n,m' \oplus n} = q_m \qquad (m \neq 0). \tag{20}$$

When the $(N-1)$ equations composed by (20) is non-singular, the solution of the $(N-1)$ taps, $\{D_{n,m' \oplus n}\}$, is unique for a certain $n$. The equation (20) also reveals that the set of the $(N-1)$ values $\{D_{n,m' \oplus n}\}$ with $m' = 1, \cdots, N-1$ is the same for any $n$. Denoting $D_{n,m' \oplus n} = d_{m'}$, the Wiener prediction (13) can be reformulated by

$$\hat{e}_n = \sum_{m'=1}^{N-1} d_{m'} e_{n \oplus m'}, \tag{21}$$

where the optimal Wiener taps $\{d_{m'}\}$ can be solved from

$$\sum_{m'=1}^{N-1} q_{m \oplus m'} d_{m'} = q_m \tag{22}$$

for $m \in [1, N-1]$. Note that the optimal Wiener prediction in (21) is conducted by a dyadic convolution, instead of a linear convolution as applied in conventional predictions. This filter structure arises because of the mechanism of causing the residual ISI and the correlated noise in (6).

### C. Wiener filter with reduced order

Finding the coefficients $d_{m'}$ from (22) is equivalent to solve the linear system of $N-1$ equations, which requires a complex computation for a large value of $N$. In order to reduce the complexity, the filter can be redesigned starting from (21) by reducing the number of taps. To do so, the ideal way is to retain only the $B$ most significant taps and neglect the others. However, currently there is no straightforward way to immediately sort out the significance in practice. Considering the structure of the feedback matrix, the most convenient way is to restrict $\{d_{m'}\}$ to be zero for $m' > B$. Then the resulting estimate of the $n$th entry of $\hat{\boldsymbol{e}}$ is written as

$$\hat{e}_n = \sum_{m'=1}^{B} d_{m'} e_{n \oplus m'}, \tag{23}$$

where $\{d_{m'}\}$ can be obtained by solving the $B$ equations

$$\sum_{m'=1}^{B} q_{m \oplus m'} d_{m'} = q_m \tag{24}$$

for non-negative integers $m$, $n$, $s$. Another important property of modulo-2 addition is that if $m \oplus n = s$, then $m = n \oplus s$ is valid.

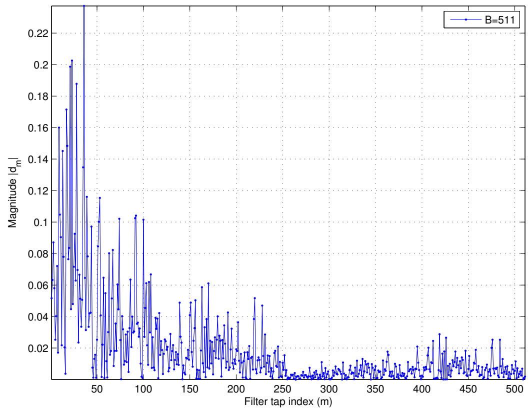


Fig. 2. The estimated feedback coefficients for a typical radio channel.

for $m \in [1, B]$.

Now we examine the significance of the selected $B$ taps, which determines how accurate is the estimation of the error signal in decision variables and eventually the system performance. A lot of computer simulations indicate that the magnitudes of FBE coefficients $\{d_m\}$ are in a decreasing trend for an exponential decaying radio channel. For instance, Fig.2 depicts the magnitudes of the estimated feedback coefficients for a typical radio channel, where the FBE filter is in full length, i.e. $B = N - 1 = 511$, and the perfect decisions are used for the estimation. Here, the first 50 taps falls into the group of the most significant coefficients. Therefore, using a limited number of taps according to (23) might give a sufficient performance, as shown by simulations in Section V, with a fairly acceptable complexity.

In addition, it is seen from (11) and (24) that the optimal coefficients of FFE are not dependent on the feedback coefficients. This indicates that the number change of the feedback taps will not affect the FFE unit, in contrast to the decision-directed DFE. This provides flexibility and adaptivity to practical systems.

## V. Simulation Results

In this section, baseband equivalent simulations are conducted to evaluate the performance of the proposed DFE for synchronous MC-CDMA systems. A Rician channel is simulated with the first tap fixed and other taps following Rayleigh fading distributions whose variances are exponentially decaying. The Rician $K$-factor, the root-mean-squared delay spread and the maximum excess delay are 1, 7.5 ns and 75 ns, respectively. The channel parameters are consistent with the measured LOS indoor channels configured with omnidirectional antennas in the frequency band of 60 GHz [15]. The simulated bandwidth is 1.75 GHz and the data block length is 512. Here the cyclic prefix is set to be 1/4 of the symbol duration, which is large enough to absorb the ISI between data blocks. The channel is perfectly known in the receiver and the received signal is perfectly synchronized in time and frequency.

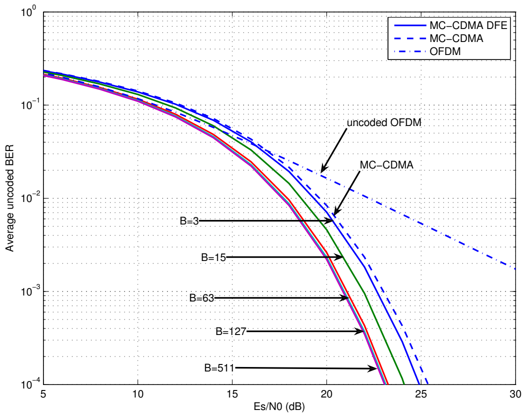


Fig. 3. Average uncoded BER performance with perfect feedback.

### A. *Uncoded performance with ideal feedback*

Fig.3 depicts the average uncoded BER performance for 16-QAM with Gray bit-mapping as a function of the carrier-to-noise ratio in terms of $E_s/N_0$ (energy per symbol over the noise density). To explore the performance limit, the ideal feedback is applied to predict the signal error. As a reference, the BER performance of the conventional OFDM and MMSE-based MC-CDMA is also shown. From this figure, one can see that the proposed DFE scheme provides visible performance gains at practical SNR ($E_s/N_0 > 10$ dB) relative to the conventional MMSE-based MC-CDMA. For a small tap order ($B = 3$), the proposed DFE scheme has the advantage of about 0.4 dB gain, at the target BER $1 \times 10^{-3}$, compared with the MMSE-based MC-CDMA. Raising the tap order leads to larger improvements. For instance, the proposed DFE scheme has about 1.1 and 1.9 dB gains for $B = 15$ and 63, respectively. It is also shown that for the tap order $B > 63$, the gain margin becomes limited, which can be explained by the fact that the feedback coefficients for $B > 63$ have negligible values, as observed from Fig.2. For the full order DFE with $B = 511$, the gain is about 2.1 dB.

## VI. Conclusions

In this paper, a predictive DFE structure was used and the optimal MMSE-DFE equalizer was designed for the MC-CDMA signal detection. While the feedforward stage was equivalent to the MMSE equalizer in the conventional MC-CDMA, a Wiener filter was designed in the feedback stage to suppress the residual ISI and correlated noise caused by the channel equalization and code despreading in the feedforward stage. Simulations showed that the proposed DFE scheme achieves a significant performance improvement, up to 2.1 dB gain, over the conventional MMSE-based MC-CDMA detection. This largely removes the SNR penalty between MC-CDMA and ideally coded OFDM observed in [2].

## References

[1] N. Yee and J.P. Linnartz and G. Fettweis, "Multi-carrier CDMA in indoor wireless radio networks," in *Proc. IEEE PIMRC'93*, 1993, pp. 109–113.

[2] J. P. M. G. Linnartz, "Performance Analysis of Synchronous MC-CDMA in Mobile Rayleigh channel with both Delay and Doppler Spreads," *IEEE Trans. Veh. Technol.*, vol. 50, no. 6, pp. 1375–1387, Nov. 2001.

[3] K. Kaiser, "On the performance of different detection techniques for OFDM-CDMA in fading channels," in *IEEE ICC '95*, June 1995, pp. 2059–2063.

[4] N. Yee and J.P. Linnartz, "Wiener Filtering of Multi-carrier CDMA in Rayleigh Fading Channel," in *Proc. IEEE PIMRC'94*, 1994, pp. 1344–1347.

[5] N. Yee and J. Linnartz, "Multi-Camer CDMA in an Indoor Wireless Radio Channel," Electronics Research Laboratory, University of Califomia, Berkeley, Tech. Rep., 1994.

[6] J. Proakis, *Digital communications*. McGraw-Hill, 2001.

[7] N. Benvenuto and S. Tomasin, "On the comparison between OFDM and single carrier with a DFE using a frequency domain feedforward filter," *IEEE Trans. Commun.*, vol. 50, no. 6, pp. 947–955, 2002.

[8] Y. Zhu and K. B. Letaief, "Single carrier frequency domain equalization with noise prediction for broadband wireless systems," in *IEEE Globecom'04*, Dec. 2004, pp. 3098–3102.

[9] Y. Sun and L. Tong, "Channel equalization using one-tap DFE for wireless OFDM systems with ICI and ISI," in *SPAWC'99*, May 1999, pp. 146–149.

[10] C. Belfiore and J. Park, "Decision feedback equalization," *Proc. IEEE*, vol. 67, pp. 1143–1156, Aug. 1979.

[11] M.V. Eyuboğlu, "Detection of coded modulation signals on linear, severely distorted channels using decision-feedback noise prediction with interleaving," *IEEE Trans. Commun.*, vol. 36, no. 4, pp. 401–409, Apr. 1988.

[12] K. Zhou, J. Proakis, and F. Ling, "Decision-Feedback Equalization of Time-Dispersive Channels with Coded Modulation," *IEEE Trans. Commun.*, vol. 38, no. 1, pp. 18–24, Jan. 1990.

[13] J. Hagenauer, "The Turbo Principle: Tutorial Introduction and State of the Art," in *Proc. of Int. Symposium on Turbo-Codes*, Sept. 1997, pp. 1–11.

[14] A. Tanenbaum, *Computer Networks*. Prentice Hall, 1996.

[15] H. Yang and P.F.M. Smulders and M.H.A.J. Herben, "Channel Characteristics and Transmission Performance for Various Channel Configurations at 60 GHz," *EURASIP Journal on Wireless Communications and Networking, Article ID 19613*, 2007.